The Scattering of a TM Surface Wave by a Perfectly Conducting Strip

E. S. GILLESPIE, MEMBER, IEEE, AND J. J. GUSTINCIC, MEMBER, IEEE

Abstract—The scattering of a TM surface wave by a metallic strip above a dielectric-clad ground plane is investigated both theoretically and experimentally. An expression for the Green's function which can be evaluated numerically is developed for the usual case for which the energy of the incident surface wave is "lightly trapped" by the dielectric. Using this expression, a variational formula for the reflection coefficient of the strip is developed, and the Rayleigh-Ritz technique is applied to yield approximate values for the reflection coefficient and surface currents of the strip.

Numerical results are presented and compared with experimental values measured on a polystyrene-coated aluminum table. Strips measuring up to one wavelength in width positioned up to one wavelength above the dielectric are considered, and agreement between theory and experiment is found to be good.

A thorough description of the experimental apparatus and techniques is presented.

Introduction

DURING the past fifteen years there has been a considerable amount of work reported in the literature concerned with various aspects of electromagnetic surface waves. Much of this work has now been compiled in texts, notably those by Barlow and Brown [1], Collin [2], and Jasik [3]. Although surface wave phenomena have been investigated extensively, little has been done toward solving, theoretically, the scattering problem associated with obstacles near such a transmission system. King and Schlesinger [4] have made measurements of the reflection coefficients of obstacles near a dielectric image line, as have DuHamel and Duncan [5]. The latter group derived an integral expression for the reflection coefficient, but it was only incidental to their experimental procedure. Sharma [6] has considered the case of a thin conducting strip normal to a surface wave system; however, he restricted his analysis to the case in which the lower edge of the strip was attached to the surface. Also, he obtained only the magnitude of the transmission coefficient and made no estimate of its phase angle.

A theoretical study of the scattering of obstacles near a surface waveguide is important from several points of view. The microwave engineer has the problem of impedance matching with minimum loss due to radiation. The use of obstacles is, of course, a standard technique in closed waveguides [7]. It would be highly desirable to extend this technique to open guides as well. However, the antenna engineer is interested not only in the matching problem, but at the same time in controlling the radiation in such a way as to produce a desired radiation pattern. The judicious use of obstacles provides a means of accomplishing this control. DuHamel and Duncan [8] have been successful in developing such a technique through the use of experimental methods. For these reasons it was decided to investigate the scattering of a plane surface wave by a thin metallic strip.

Manuscript received December 14, 1964; revised March 19, 1965. The work reported in this paper was supported in part by the National Aeronautics and Space Administration under NASA research grant No. NsG 237.
E. S. Gillespie is with The San Fernando Valley State College, Northridge, Calif. He was formerly with the Institute of Geophysics and Planetary Physics, University of California, Los Angeles, Calif.
J. J. Gustincic is with the Department of Electrical Engineering, University of California, Los Angeles, Calif.

Discussion of the Problem

The problem to be considered is that of determining the reflection coefficient of a perfectly conducting, indefinitely thin strip located an artibrary distance above a dielectric-coated ground plane which supports a plane TM surface wave. The thickness of the dielectric is adjusted to permit only the lowest-order TM surface wave mode to propagate. The geometry of the problem in shown in Fig. 1.

The field components of the incident surface wave can be written [3] in complex form as

$$E_y^i = Ae^{-\alpha_0 y - j\beta_0 z} \tag{1}$$

$$E_z^i = j\frac{\alpha_0 A}{\beta_0} e^{-\alpha_0 y - j\beta_0 z} \tag{2}$$

$$H_x^i = \frac{\beta_0 A}{\omega\epsilon_0} e^{-\alpha_0 y - j\beta_0 z}. \tag{3}$$

The attenuation constant α_0 and propagation constant β_0 are related as follows:

$$\beta_0^2 = k_0^2 + \alpha_0^2 \tag{4}$$

where k_0 is the free-space wave number.

Referring to Fig. 1, the incident field induces an electric current on the surface of the strip, which is only y directed. This current sheet, with a density $J(y)\boldsymbol{a}_y$ per unit length in the x direction, radiates a scattered field $\boldsymbol{E}^s$, $\boldsymbol{H}^s$.

The total scattered electric field at some arbitrary point above the guiding surface consists of three parts: a direct radiation field from the scatterer, a reflected radiation field from the surface, and a scattered surface wave. The ratio of the transverse electric field of the backscattered surface wave to the transverse electric field of the incident wave will be defined as the reflec-

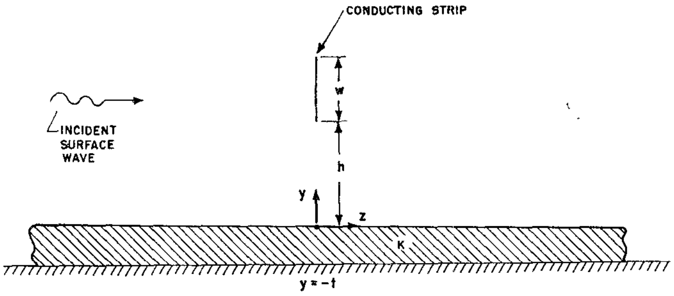

Fig. 1. Guiding surface and strip scatterer.

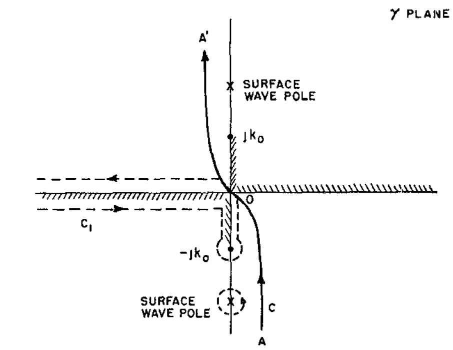

Fig. 2. Proper branch cuts and the contours of integration.

tion coefficient of the strip. The transverse component of electric field of the reflected surface wave $(E_y^s)_{sw}$ can be related to the incident field by

$$(E_y^s)_{sw} = \Gamma E_y^i \tag{5}$$

in which Γ is the reflection coefficient.

The total magnetic vector potential for the induced current distribution has only a y component, which is given by

$$A_y(y, z) = \int_{\text{strip}} G(y, y'; z) J(y') dy' \tag{6}$$

where $G(y, y'; z)$ is the Green's function for the problem. The scattered transverse electric field is then given by

$$E_y^s = \frac{1}{j\omega\epsilon}\left(k^2 + \frac{\partial^2}{\partial y^2}\right) A_y. \tag{7}$$

The Green's function can be constructed directly by following the procedure outlined by Collin [2], with the result

$$G(y, y'; z) = -j\frac{\mu_0}{4}\left[H_0^{(2)}\left(k_0\sqrt{(y-y')^2+z^2}\right) + g(y+y', z)\right] \tag{8}$$

in which

$$g(y + y', z) = \frac{1}{j\pi}\int_C \frac{R}{l} e^{-jl|y+y'|-\gamma z} d\gamma. \tag{9}$$

In (9) l is taken to be that branch of $\sqrt{\gamma^2+k_0^2}$ for which $\text{Im } l<0$ and R is the reflection coefficients for the plane waves which make up (9), that is,

$$R = \frac{l\kappa + b \tan bt}{l\kappa - b \tan bt} \tag{10}$$

where $b=\sqrt{\gamma^2+\kappa k_0^2}$. The contour C and the branch cuts of γ are shown in Fig. 2.

An expression for the reflection coefficient in terms of the induced current distribution can be obtained directly from (6). Unfortunately, this current distribution is not known; therefore, a variational method will be used to obtain a stationary expression for Γ in terms of the unknown current distribution. The procedure is similar to that used to determine equivalent circuit parameters for diaphragms in waveguides [2], [7], but the problem is more complicated for an open surface wave system than for a closed waveguide structure because there exists in the former—in addition to a number of discrete modes—a continuous spectrum of scattered radiation.

The first term in (8) leads to the direct radiation from a line dipole source (9), and the second integral describes that radiation field which is reflected from the ground plane and modified by the presence of the dielectric coating. For $z<0$, the contour C can be warped into the contour C_1 in the left-half plane, as shown in Fig. 2. By doing this it is seen that $g(y+y', z)$ consists of the sum of a reflected surface wave due to the pole at $\gamma=-j\beta_0$ and a radiation field obtained from the integration around the branch cut.

The transverse electric field due to the reflected surface wave term is then

$$(E_y^s)_{sw} = \frac{-\beta_0^2}{2\omega\epsilon_0\alpha_0}\left[\text{Res}\,[R]_{\gamma=-j\beta_0}\int_{\text{strip}} J(y')e^{-\alpha_0 y'}dy'\right] \cdot e^{-\alpha_0 y+j\beta_0 z}. \tag{11}$$

For convenience the amplitude of the incident wave is adjusted to unity, and the reflection coefficient defined by (5) can be written as

$$\Gamma = \left[\frac{R_0\beta_0}{2\omega\epsilon_0}\right]\int_{\text{strip}} e^{-\alpha_0 y'} J(y') dy' \tag{12}$$

where R_0 is obtained from the evaluation of the residue of R, and is given by

$$R_0 = \frac{-2\alpha_0}{1 + \dfrac{\alpha_0[\kappa\alpha_0 + t(\kappa^2-1)\alpha_0^2 + t(\kappa-1)k_0^2]}{\kappa[(\kappa-1)k_0^2 - \alpha_0^2]}}. \tag{13}$$

This result could have been obtained by using the reciprocity theorem [1], [8], and [10].

If the current distribution $J(y)$ were known, the reflection coefficient could be computed from (12). Attempts have been made to approximate the current by assuming it to be of the same form as the short-circuit distribution [1], [10]. The results were in error by a factor of about 2 for strips with a width of one wavelength. Also, no information on the phase of the reflection coefficient was obtained.

Mathematical Formulation

To determine the scattering properties of the strip under consideration, it is only necessary to know the tangential component of the electric field in the plane of the strip. Therefore, z is set equal to zero in (9), and only the expression

$$g(y, 0) = \frac{1}{j\pi}\int_C \frac{R}{l} e^{-jl_y d\gamma}$$

need be investigated. In the Appendix this integral is put into the following form:

$$g(y, 0) = -R_0 L e^{-\alpha_0 y} + G_1(y)$$

where

$$G_1(y) = R_0 \int_0^y e^{-\alpha_0(y-y')} H_0^{(2)}(k_0 y')dy' + \left(\frac{\kappa - 1}{\kappa + 1}\right) H_0^{(2)}(k_0 y) - \frac{4\kappa}{(\kappa^2 - 1)} \sum_{m=1}^{\infty} \left[\frac{1-\kappa}{1+\kappa}\right]^m H_0^{(2)}(k_0 y + 2mk_0 t) \quad (14)$$

and L is the Laplace transform of the Hankel function, with the transform variable set equal to $-\alpha_0$:

$$L = \int_0^\infty e^{-s_0 y'} H_0^{(2)}(k_0 y')dy' \Big|_{s_0 \to -\alpha_0} = \frac{1}{\beta_0}\left[1 + j\frac{2}{\pi} \ln\left(\frac{\beta_0 + \alpha_0}{k_0}\right)\right]. \quad (15)$$

This formulation is subject to the condition that

$$\sqrt{\kappa - 1}\, k_0 t \ll \frac{\pi}{2} \cdot \quad (16)$$

This condition is satisfied in those cases for which the energy of the surface wave is "lightly trapped," that is, contained mostly in the air immediately above the dielectric rather than in the dielectric itself. This is true for most practical surface wave systems where it is desirable to minimize losses.

The representation (14) is now well-suited to numerical calculation. The integration in this expression extends over a finite interval which is small for low strips, and the sum converges fairly rapidly because of the factor $(1-\kappa/1+\kappa)^m$. The sum in (14) is due to the "leaky-wave" poles of $R(s)$ and can be interpreted physically as an infinite number of image sources placed at multiples of $2t$ below the usual image point. Specifically, the reflected radiation at y due to a point source at y' is $g(y+y', 0)$. Thus, when y is replaced by $y+y'$ in (14), the Hankel function in the sum has as its argument $k_0\{(y+t)+(y'+t+2t[m-1])\}$. The first image source is then at $y=-(y'+t)$ and succeeding sources are at $y=-\{y'+t+2t(m-1)\}$, with decreasing amplitudes given by

$$\left(\frac{1-\kappa}{1+\kappa}\right)^m.$$

Note that as κ approaches unity and the dielectric disappears, all terms in (14) vanish, except for the $m=1$ term which becomes

$$H_0^{(2)}(k_0[y + y' + 2t]),$$

and this term is seen to be just the usual image source for reflection by a perfectly conducting ground plane.

A variational expression from which the reflection coefficient Γ can be calculated will now be developed. From (8) and (14), the Green's function for the problem can be written as

$$G(y, y'; 0) = -j\frac{\mu_0}{4}\left[G_1(|y + y'|) + G_2(|y - y'|) - R_0 L e^{-\alpha_0(y+y')}\right] \quad (17)$$

where

$$G_2(y) = H_0^{(2)}(k_0 y)$$

with $G_1(y)$ and L given by (14) and (15), respectively. At the strip, the scattered field must cancel the y component of incident electric field, and thus (6), (7), and (17) yield

$$E_y^s(y, 0) = -e^{-\alpha_0 y} = -\beta_0 R_0 L e^{-\alpha_0 y}\int_{\text{strip}} e^{-\alpha_0 y'} J(y')dy' - \frac{1}{4\omega\epsilon_0}\left(k_0^2 + \frac{\partial^2}{\partial y^2}\right)\int_{\text{strip}} \cdot [G_1(|y + y'|) + G_2(|y - y'|)]J(y')dy'. \quad (18)$$

Notice that the second derivative acting on the function $G_1(|y+y'|)$ produces a singularity that requires interpretation of the integral in (18) in a principal value sense and renders the integration impractical from the standpoint of numerical calculation. This difficulty can be overcome by recognizing that

$$\frac{\partial^2}{\partial y^2} G_1(|y + y'|) = -\frac{\partial^2}{\partial y \partial y'} G_1(|y + y'|)$$
$$\frac{\partial^2}{\partial y^2} G_2(|y - y'|) = \frac{\partial^2}{\partial y \partial y'} G_2(|y - y'|). \quad (19)$$

Equation (18) is next multiplied through by $J(y)$ and integrated over the strip. Making use of (19), the terms involving G_1 and G_2 can be integrated by parts twice, once with respect to y and once with respect to y'. Since the edge condition requires that $J(y)$ vanish at both edges of the strip, the process yields

$$\beta_0^2 R_0 L \left[\int_{\text{strip}} J(y')e^{-\alpha_0 y'}dy' \right]^2 + \int_{\text{strip}} J(y')e^{-\alpha_0 y'}dy'$$
$$= \frac{1}{4\omega\epsilon_0} \iint_{\text{strip}} [I(y, y')G_1(|y + y'|)$$
$$+ \bar{I}(y, y')G_2(|y - y'|)]dydy' \quad (20)$$

where

$$I(y, y') = J(y)J(y') - k_0^2 \frac{dJ(y)}{dy} \frac{dJ(y')}{dy'}$$
$$\bar{I}(y, y') = J(y)J(y') + k_0^2 \frac{dJ(y)}{dy} \frac{dJ(y')}{dy'} .$$

Dividing (20) through by

$$\frac{R_0\beta_0}{2\omega\epsilon_0} \left[\int_{\text{strip}} J(y')e^{-\alpha_0 y'}dy' \right]^2$$

and recalling the definition of Γ given by (12) yields the following expression:

$$\frac{(L\beta_0/2)\Gamma + 1}{\Gamma} = \frac{\iint_{\text{strip}} [I(y, y')G_1(|y + y'|) + \bar{I}(y, y')G_2(|y - y'|)]dydy'}{2\beta_0 R_0 \left[\int_{\text{strip}} J(y')e^{-\alpha_0 y'}dy' \right]^2} \quad (21)$$

in which L is given by (15) and R_0 by (13). It can be directly verified that (21) is sationary with respect to a first-order variation in $J(y)$ and is dependent only on its functional form. (See, for example, Collin [2], pp. 331–332.)

Numerical Calculations and Discussion of Results

It was decided that instead of merely evaluating (26) with a single judicious approximation for the unknown current, the current would be expanded in a set of functions and the Rayleigh-Ritz procedure employed. The additional integrations involved in this latter technique pose no real increase in complexity, and at the same time the process has the advantage of giving a description of the unknown current $J(y)$.

The following truncated Fourier sine series with complex coefficients was used to approximate the current

$$J(y) = \sum_{m=1}^{N} a_m \sin\left[\frac{m\pi}{w}(y - h)\right] \quad h \le y \le h + w. \quad (22)$$

This expression was then substituted into the stationary functional (21), and derivatives were taken with respect to the a_m according to the usual Rayleigh-Ritz method. Approximate values for Γ were then computed, as well as values for the a_m. The rapid convergence of these values with increasing N, along with the resulting close agreement between the computed values of Γ and the experimental ones, indicated that this procedure was satisfactory.

The integrals in (21) were evaluated by breaking up each strip into from 100 to 200 equal intervals and summing the values of the integrand at the center of each interval. For those intervals in which $G_2(|y-y'|)$ had a logarithmic singularity, the integration over the interval was performed analytically by using the small argument approximation for the Hankel function and assuming that $I(y, y')$ would remain constant over the interval. Increasing the number of intervals changed the final result by only a fraction of a per cent, indicating that the integration scheme was sufficiently accurate.

Since the Green's function for the reflected radiation field given by (14) appears as an integrand in (21), this field was computed with greater care in order to minimize any compounding of error. The sum in (14) was carried out to ten terms, and the integration was performed using Simpson's rule with 100 intervals per unit of argument.

All calculations were performed by an IBM 7094 at the computing facility of the University of California at Los Angeles. The results of the computations for Γ are presented in Table I.

Typical computed values of the magnitude and phase angle of the reflection coefficient for various heights above the surface are displayed graphically in Figs. 3 and 4, respectively. Measured values are also shown. The correspondence between the theoretical and the experimental data is quite good. Note that as the width of the strip is increased, the magnitude of the reflection coefficient increases to a maximum at a width slightly greater than a half wavelength. The magnitude then begins to decrease for widths approaching one wavelength. The decrease is more pronounced for the lower heights where the image fields are the strongest. This effect shows up in both the theoretical and the experimental data and is thought to be the start of an oscillatory behavior which is typical of diffraction phenomena.

The phase angle of the reflection coefficient appears to be almost independent of the height of the strip. For

TABLE I
COMPUTED REFLECTION COEFFICIENTS

Strip Height (k_0h)	Strip Widths (k_0w) 0.50	1.00	1.25	1.80	2.20
0.50	0.028/−91°	0.11/−99°	0.17/−103°	0.32/−114°	0.45/−124°
1.50	0.020/−91°	0.08/−96°	0.12/−99°	0.25/−110°	0.37/−122°
2.51	0.013/−92°	0.05/−96°	0.08/−100°	0.18/−113°	0.25/−127°
3.77	0.008/−91°	0.03/−96°	0.05/−100°	0.10/−112°	0.15/−124°
5.02	0.005/−91°	0.02/−96°	0.03/−100°	0.07/−112°	0.10/−125°

Strip Height (k_0h)	Strip Widths (k_0w) 2.50	2.80	3.20	3.76	4.92
0.50	0.55/−130°	0.63/−138°	0.72/−147°	0.77/−159°	0.72/−170°
1.50	0.45/−133°	0.51/−144°	0.54/−156°	0.52/−166°	0.49/−172°
2.51	0.29/−137°	0.32/−146°	0.33/−155°	0.34/−163°	0.33/−170°
3.77	0.18/−134°	0.20/−142°	0.22/−153°	0.22/−163°	0.21/−171°
5.02	0.12/−135°	0.13/−145°	0.14/−155°	0.14/−165°	0.13/−171°

narrow strips (less than a quarter wavelength) the impedance of the strip is almost completely reactive. This implies that the loss due to radiation is small. As the strip width approaches zero, the phase angle asymptotically approaches −90° and the strip becomes equivalent to a shunt capacitance. As the strip width increases, the phase angle asymptotically approaches −180° and the strip becomes resistive. If the reflection coefficient of a particular strip is plotted as a function of height above the surface, the effect of the exponential decay of the incident surface wave field is clearly evident (Fig. 5).

All of the computed results that have been presented were obtained using four terms in the current series. When only two terms were used, it was found that for the narrower strips the correspondence between the theoretical and the experimental results was not as good as desired. It was determined that for the narrow strips the third harmonic of the current representation had a significant value and could not be neglected. The fifth- and higher-order harmonics were found to be negligible.

The higher-order complex coefficients of the current spectrum are shown in Fig. 6 for a fixed value of strip height ($k_0h=1.5$). These amplitudes are normalized to the complex value of a_1. Note that of the higher harmonics for the widest strip, the second harmonic is dominant. As the strip is made narrower, the second harmonic decreases and the third harmonic increases until it eventually predominates. Also, it is significant that for the wider strips the complex coefficients are out of phase with one another; but for the narrow strips, all components are in phase. This behavior is readily explained in physical terms. When the strip is narrow and the fields are essentially uniform over it, the current should also be fairly uniform in both magnitude and phase. This would also indicate a large third-harmonic content since this harmonic is symmetric over the strip. For wide strips, the current should exhibit some asymmetry as the incident field decays nonuniformly from bottom to top of the strip, thus requiring a large second harmonic. Also, phase variations are to be expected for wide strips since radiation is high and the current should have some of the character of the scattered radiation field.

The components of the computed current can be summed so that the approximate current distribution along the strip can be determined. This has been done for three different strip widths and the results are shown in Fig. 7(a). Note that for the widest strip the exponential decay of the incident field has a pronounced effect upon the current distribution. Of interest also is the variation of phase over the strip. Only the phase angle for the widest strip is shown in Fig. 7(b) since the phase was almost constant over the width of the narrower strips, whereas it varied approximately 60° over the widest strip. This could easily account for the fact that when the short-circuit current—which predicts no phase variation—is used in the equation for the reflection coefficient, the results are in substantial error [1]. The current distributions determined from this analysis can be used to compute the radiated field; hence, the total scattered field can be determined. This work is under way at the present time and will be reported later.

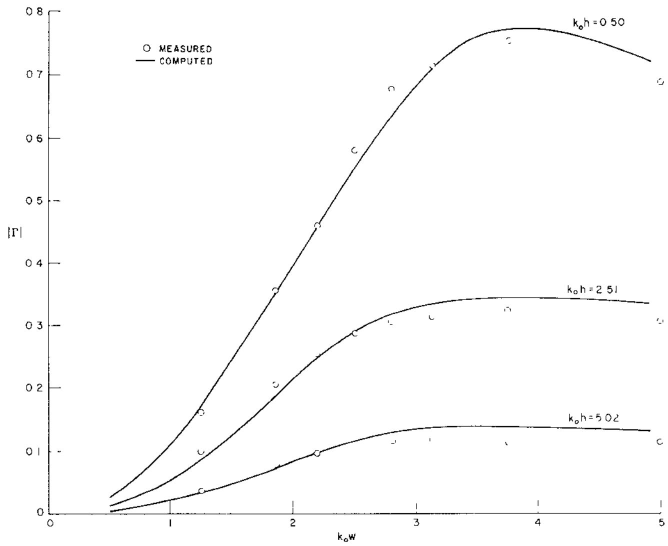

Fig. 3. Magnitude of the reflection coefficient for various heights as a function of width.

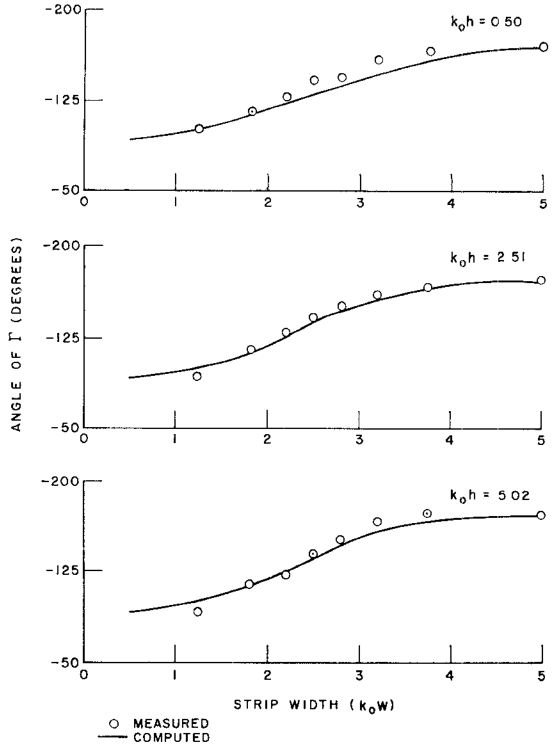

Fig. 4. Phase angle of the reflection coefficient for various heights as a function of width.

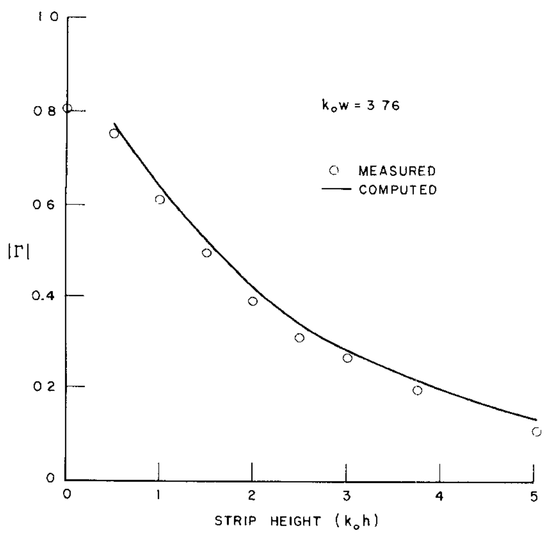

Fig. 5. Magnitude of the reflection coefficient as a function of height with $k_0w = 3.76$.

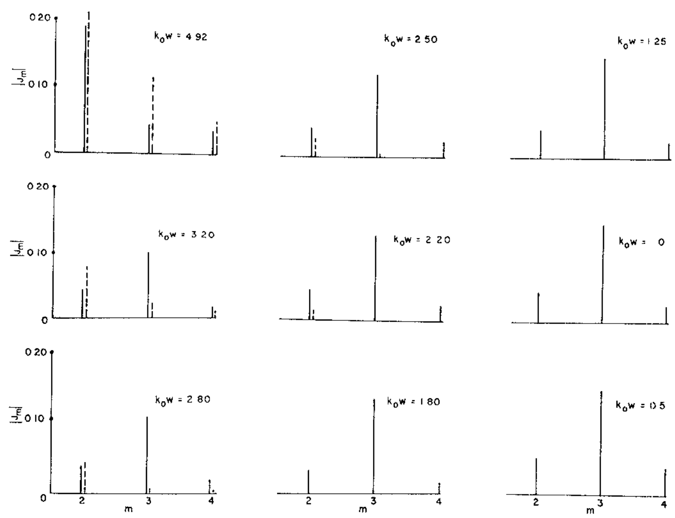

Fig. 6. Higher-order complex coefficients of the computed current for various widths with $k_0h = 1.50$ (——— real part; - - - imaginary part).

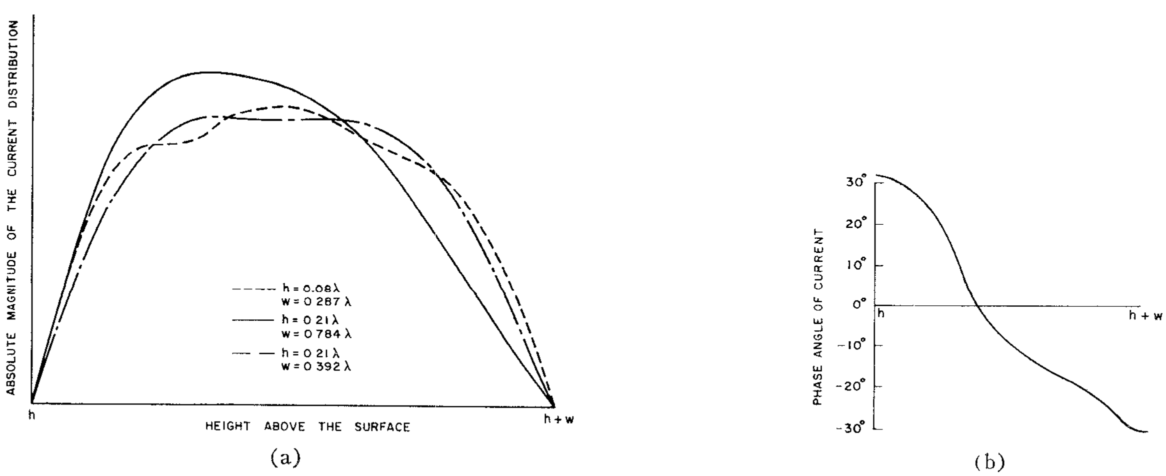

Fig. 7. (a) Absolute magnitude of the computed current distribution for various strip heights and widths. (b) Phase angle of the computed current distribution for a strip of width 0.392 λ and height 0.21 λ (see text).

Experimental Study

At the outset of the study it was recognized that it was impossible to duplicate experimentally the two-dimensional problem that was posed. It was possible, however, to achieve a high degree of approximation by use of a surface wave system of sufficient width. After reviewing the reported work of other researchers, particularly that of Cullen [11] and Rich [12], it was decided that a table with a width of ten wavelengths or more is sufficient. The width chosen was 18.25 wavelengths, which proved more than adequate.

The length of the table was chosen so that the surface wave field would not be contaminated, at the scatterer under test, by direct radiation from the launcher. Taking advantage of the experience of Rich [12], whose apparatus was similar to ours, we chose a table length of 7 feet. The table itself was constructed by bonding together two sheets of aluminum. The thicknesses of the two sheets were 9/64 inch and 3/4 inch, respectively. These dimensions were selected in order than a standard tunable probe might be used in the slotted section. Also, by using thick aluminum, the mounting of auxiliary mechanisms—such as the sliding termination—was greatly simplified.

The surface wave launcher used was a standard double-cheese design. A sketch of the experimental apparatus is shown in Fig. 8.

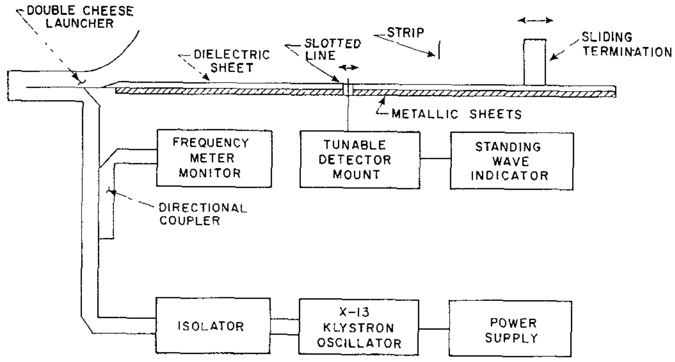

Fig. 8. Block diagram of experimental apparatus.

When the thickness of the plastic and its dielectric constant are known, the decay factor α_0 can be computed for the surface wave field using the approximate formula [2]

$$\alpha_0 = k_0^2\left(\frac{\kappa - 1}{\kappa}\right)t.$$

For this study the frequency was chosen to be 9375 Mc. The thickness of the plastic was 1/16 inch, and its dielectric constant was 2.54. Substituting these quantities in the foregoing equation revealed that

$$\alpha_0 = 0.94/\text{inch}.$$

Using this value for α_0, a computation was made of the relative field as a function of height above the reactive surface. α_0 was also determined experimentally using a tapered probe. The experimental value was in close agreement with the computed value.

Since the TM mode excites only a longitudinal current in the metallic surface, it was possible to construct a slotted section in the table with a minimal perturbation of the field. The required short circuit was accomplished by fastening an alclad aluminum plate to aluminum angle so that the assembly was self-supporting and the plate stood vertical. A 6-inch height was adequate for the short circuit.

In order to eliminate the need for a perfect termination for the surface wave system, the sliding termination method of impedance measurement [13], [14] was adopted. The slotted section was located approximately 22 wavelengths from the aperture of the surface wave launcher. The strip under test was located approximately 20 wavelengths from the slotted section. For the measurements reported here, the termination was located approximately 12 wavelengths from the strip and the required movement was only 0.6 inch. The increments were taken to be about 0.1 inch which represents six measurements for each strip position.

The carriage for the slotted section probe was simply an aluminum block machined to accommodate the body of the probe assembly. A rectangular-shaped hole was milled into the bottom sheet so that the carriage block could be inserted into it with a sliding fit. A slot 0.124 inch wide was milled into the top sheet so that its center line coincided with the line formed by the motion of the probe. This width was chosen to accommodate the outer conductor of the probe, as in standard waveguide slotted sections. The corresponding slot in the plastic was made 0.080 inch wide. The length of the slot was 2.65 inches which allowed a probe movement of slightly more than two wavelengths. The carriage was moved by use of a rack gear and its mating gear. The position of the carriage was determined by a dial indicator which could be read to 0.001 inch.

The sliding termination consisted of a slab of absorbing material bonded to an aluminum plate. The material was 5 inches high and extended across the full width of the table. Care was taken to insure that this assembly was at all times perpendicular to the table and to the direction of propagation of the surface wave. An assembly was designed which allowed the termination to be adjusted by a single precision worm gear located under the table. The position of the termination was obtained from a dial indicator. The termination had a mismatch of 1.3 to 1, and a measurement of its impedance as a function of its position revealed that the residual impedance of the table was negligible.

The strips used for these measurements were standard blued-steel clock springs which are available in various widths. The thickness of these strips was 0.10

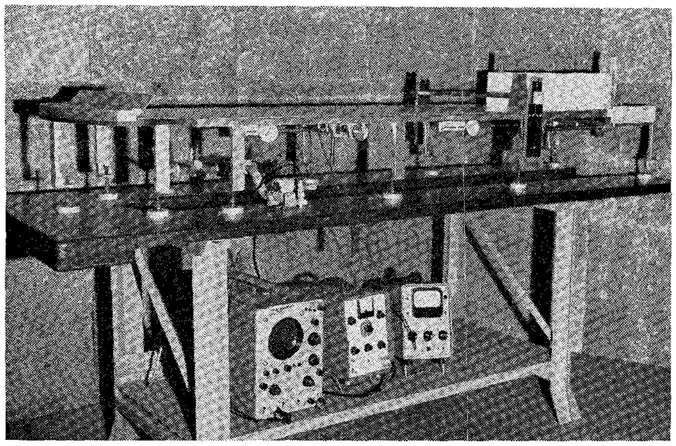

Fig. 9. Photograph of experimental apparatus.

inch. The strips were gold-plated to insure high conductivity. While being measured, each of the strips was held under tension between two plastic vertical posts. The strips were pivoted at each end to prevent twisting as tension was applied. The strips were continuously adjustable in vertical position to about 5 inches above the plastic surface. Again care was exercised to insure that the strip was perpendicular to the surface and to the direction of propagation of the surface wave.

A block diagram of the instrumentation is also shown in Fig. 8, and the completed apparatus is shown in Fig. 9. The completed assembly was considered to be highly satisfactory. Measured values of reflection coefficient for various strip widths and heights are presented in Table II.

TABLE II
MEASURED REFLECTION COEFFICIENTS

Strip Height (k_0h)	Strip Widths (k_0w)			
	1.25	1.85	2.20	2.52
0	$0.28\angle -113°$	$0.48\angle -137°$	$0.55\angle -145°$	$0.61\angle -149°$
0.50	$0.21\angle -96°$	$0.38\angle -116°$	$0.50\angle -129°$	$0.58\angle -140°$
1.00	$0.16\angle -107°$	$0.35\angle -114°$	$0.46\angle -123°$	—
1.50	—	$0.31\angle -112°$	$0.40\angle -126°$	$0.46\angle -139°$
2.00	$0.12\angle -94°$	$0.25\angle -112°$	$0.32\angle -133°$	$0.37\angle -145°$
2.50	$0.10\angle -93°$	$0.21\angle -115°$	$0.26\angle -129°$	$0.29\angle -143°$
3.01	$0.06\angle -92°$	$0.17\angle -115°$	$0.20\angle -126°$	$0.23\angle -141°$
3.76	$0.05\angle -92°$	$0.12\angle -115°$	$0.15\angle -124°$	$0.17\angle -136°$
5.02	$0.03\angle -93°$	$0.08\angle -113°$	$0.09\angle -123°$	$0.11\angle -139°$
7.53	$0.02\angle -73°$	$0.03\angle -118°$	$0.03\angle -101°$	$0.04\angle -127°$

Strip Height (k_0h)	Strip Widths (k_0w)			
	2.84	3.14	3.76	5.02
0	$0.68\angle -159°$	$0.73\angle -159°$	$0.81\angle -167°$	$0.82\angle -179°$
0.50	$0.68\angle -145°$	$0.71\angle -156°$	$0.75\angle -167°$	$0.69\angle -177°$
1.00	$0.62\angle -146°$	$0.63\angle -158°$	$0.61\angle -169°$	$0.57\angle -176°$
1.50	$0.51\angle -152°$	$0.50\angle -160°$	$0.50\angle -168°$	$0.46\angle -176°$
2.00	$0.39\angle -153°$	$0.39\angle -160°$	$0.40\angle -166°$	$0.38\angle -173°$
2.50	$0.30\angle -153°$	$0.31\angle -160°$	$0.32\angle -166°$	$0.31\angle -171°$
3.01	$0.25\angle -151°$	$0.25\angle -158°$	$0.27\angle -166°$	$0.27\angle -171°$
3.76	$0.18\angle -148°$	$0.19\angle -159°$	$0.20\angle -166°$	$0.20\angle -172°$
5.02	$0.11\angle -152°$	$0.11\angle -160°$	$0.11\angle -167°$	$0.11\angle -171°$
7.53	$0.04\angle -154°$	$0.04\angle -161°$	$0.04\angle -170°$	$0.04\angle -161°$

Conclusion

The reflection coefficient of a perfectly conducting strip above a dielectric-clad ground plane supporting a plane surface wave can be computed with a high degree of accuracy using the results of the analysis reported here. Of course, the surface wave system must be such that the condition expressed by (16) holds. This condition is met in most practical surface wave systems. Hence these results are quite general.

From the analysis the current distribution has been determined to a close approximation. Therefore, the radiation field can easily be calculated.

Appendix

Evaluation of the Reflected Field Integral

The purpose is to find a more suitable representation for the integral

$$g(y, 0) = \frac{1}{j\pi}\int_C \frac{R}{l} e^{-j\gamma y} d\gamma. \tag{23}$$

The integrand of (23) is greatly complicated because of the fact that R contains γ explicitly and as such is an irrational function of the complex variable of integration γ. This condition can be resolved by making the transformation of variables

$$s = j\sqrt{\gamma^2 + k_0^2}. \tag{24}$$

Under this transformation, $s = -jl$ and the radiation condition, Im $l<0$, defines which branch of the square root in (24) constitutes a valid transformation. That is, the contour C in the γ plane must map into a contour C_2, which lies in the left-half s plane. With (24) the integral (23) becomes

$$g(y, 0) = \frac{1}{j\pi}\int_{C_2} \frac{R(s)}{\gamma(s)} e^{sy} ds \tag{25}$$

where the transformed variable and the plane-wave reflection coefficient are

$$\gamma(s) = j\sqrt{s^2 + k_0^2} \tag{26}$$

$$R(s) = \frac{\kappa s - \sqrt{\kappa k_0^2 + \gamma^2(s)}\tan\left(\sqrt{\kappa k_0^2 + \gamma^2(s)}\, t\right)}{\kappa s + \sqrt{\kappa k_0^2 + \gamma^2(s)}\tan\left(\sqrt{\kappa k_0^2 + \gamma^2(s)}\, t\right)} \cdot \tag{27}$$

The transformed contour C_2 is illustrated in Fig. 10. Note that the surface wave poles of R map into a single simple pole of $R(S)$ at $s = -\alpha_0$, and also that both segments of C (Fig. 2), $A-O$ and $O-A'$, map into the same contour C_2. Since the value of γ on $A-O$ is the negative of its value on $O-A'$, the function $\gamma(s)$ appearing in (25) is discontinuous in the s plane, undergoing a change in sign as s goes around the branch point ($s = -jk_0$) on C_2. That portion of C_2 which encompasses this branch point has been determined in the usual manner [2] by introducing losses in k_0 and then taking the limit as these losses vanish.

Note that $R(s)$ is now a rational function of s, having one surface wave pole at $s_0 \equiv -\alpha_0$ with residue R_0 as

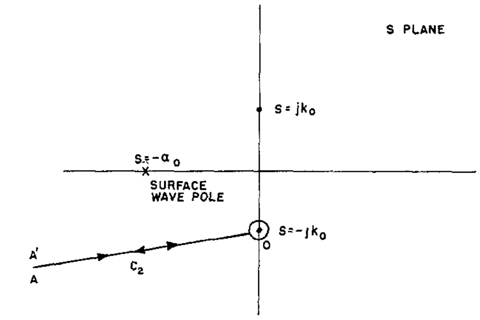

Fig. 10. Transformed contour C_2 in the s plane.

given by (13), and an infinite number of "leaky-wave" poles [15] at $s = s_n$ in the right-half s plane with residues R_n. Equally well, $R(s)$ may be expressed in terms of a partial fraction expansion

$$R(s) = R(\infty) + \sum_{n=0} \frac{R_n}{s - s_n} \cdot \tag{28}$$

That portion of C_2 labeled $O-A'$ is now warped upward and $A-O$ is warped downward, the result shown as contour C_3 in Fig. 11. This distortion is performed with $\gamma(s)$ varying continuously over one branch of the square root in (26). After C_3 has thus been established, the branch cuts shown in Fig. 11 are introduced, thereby making $\gamma(s)$ single-valued. When warping $O-A'$ up over the surface wave pole at $s = -\alpha_0$, a residue term must be subtracted from the integral and the residue evaluated with $\gamma(-\alpha_0) = +j\beta_0$. Since $\gamma(s)$ is assumed to vary continuously as $O-A'$ is moved up and away from C_2. (Recall that $O-A'$ was that portion of C for which Im $\gamma>0$.) Thus (25) becomes

$$g(y, 0) = -\frac{2R_0}{\beta_0} e^{-\alpha_0 y} + \frac{1}{2\pi j}\int_{C_3}\left(\frac{2}{\sqrt{s^2 + k_0^2}}\right) R(s) e^{sy} ds. \tag{29}$$

The second term in (29) can now be recognized as a Fourier-transform inversion integral and may be evaluated by means of the convolution theorem. The inverse transform of $2/\sqrt{s^2+k_0^2}$ with the branch cuts shown in Fig. 11 is simply the Hankel function

$$F^{-1}\left[\frac{2}{\sqrt{s^2 + k_0^2}}\right] = H_0^{(2)}(k_0 |y|) \tag{30}$$

and from (28) the inverse transform of $R(s)$ is given by

$$F^{-1}[R(s)] = R(\infty)\delta(y) + r(y)$$

where

$$r(y) = \begin{cases} R_0 e^{-\alpha_0 y} & y > 0 \\ -\sum_{n=1} R_n e^{s_n y} & y < 0. \end{cases}$$

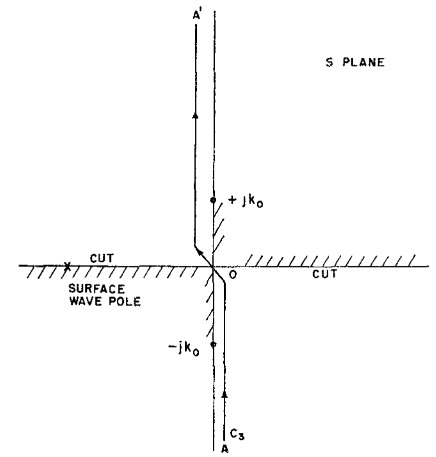

Fig. 11. Final contour C_3 shown with the branch cuts of $\gamma(s)$.

Invoking the convolution theorem yields

$$\begin{aligned}F^{-1}\left[\frac{2R(s)}{\sqrt{s^2+k_0^2}}\right] &= R(\infty)H_0^{(2)}(k_0y) + \int_{-\infty}^{+\infty} r(y-y')H_0^{(2)}(k_0|y'|)dy' \\ &= R(\infty)H_0^{(2)}(k_0y) \\ &\quad + R_0e^{-\alpha_0 y}\int_{-\infty}^{+\infty} e^{\alpha_0 y'}H_0^{(2)}(k_0|y'|)dy' \\ &\quad + \sum_{n=0} R_n\int_y^{\infty} e^{s_n(y-y')}H_0^{(2)}(k_0y')dy' \end{aligned} \tag{31}$$

where it has been assumed that

$$\int_{-\infty}^{y} e^{\alpha_0 y'}H_0^{(2)}(k_0y')dy' = \int_{-\infty}^{+\infty} e^{-s_0y'}H_0^{(2)}(k_0y')dy' - \int_y^{+\infty} e^{-s_0y'}H_0^{(2)}(k_0y')dy'.$$

Actually, the last two integrals as stated both diverge, but the assumption is valid if these integrals are interpreted as analytic continuations as s_0 approaches $-\alpha_0$ from the imaginary axis. In this light, (30) can be used to evaluate the first integral in (31) and the result substituted into (29) to yield

$$g(y,0) = R(\infty)H_0^{(2)}(k_0y) - \sum_{n=0} R_n\int_y^{\infty} e^{s_n(y-y')}H_0^{(2)}(k_0y')dy'. \tag{32}$$

It will be useful to know the asymptotic behavior of $g(y, 0)$ for large y. This behavior is easily deduced from (32). Using the asymptotic representations for the Hankel and error functions for large arguments [16], it can be shown directly that for large y

$$\int_y^{\infty} e^{-s_ny'}H_0^{(2)}(k_0y')dy' \to \frac{H_0^{(2)}(k_0y)e^{-s_ny}}{jk_0+s_n}.$$

When this result is substituted into (32), it is found that

$$\begin{aligned}g(y,0) &\to H_0^{(2)}(k_0y)\left[R(\infty)+\sum_{n=0}^{\infty}\frac{R_n}{(-jk_0)-s_n}\right] \\ &= R(-jk_0)H_0^{(2)}(k_0y).\end{aligned} \tag{33}$$

In physical terms, (33) indicates that when one gets far enough away from the dielectric in the $z=0$ plane, the indirect radiation from a current element approaches the radiation due to a simple image source modified by a factor

$$R(-jk_0) = \frac{j\sqrt{\kappa}+\tan\sqrt{\kappa}\,k_0t}{j\sqrt{\kappa}-\tan\sqrt{\kappa}\,k_0t}.$$

This factor is just the reflection coefficient for a plane wave incident normal to the dielectric.

If (32) is to be reduced further, the values of the residues R_n and the poles s_n must be determined, as shown in the following section.

Evaluation of the Poles and Residues of $R(s)$

The transformed reflection coefficient $R(s)$ given by (27) is of the form

$$R(s) = \frac{-P(-s)}{P(s)} \tag{34}$$

where

$$\begin{aligned}P(s) &= \kappa s + \sqrt{(\kappa-1)k_0^2-s^2} \\ &\quad \cdot\tan\left(\sqrt{(\kappa-1)k_0^2-s^2}\,t\right)\end{aligned} \tag{35}$$

and the poles of $R(s)$ are, of course, determined by the zeros of $P(s)$. It is convenient to make the substitution

$$z = 2t\sqrt{(\kappa-1)k_0^2-s^2}$$

or

$$s^2 = -\frac{z^2}{4t^2}\left[1-\frac{(\kappa-1)k_0^2 4t^2}{z^2}\right] \tag{36}$$

and seek the values of $z=x+jy$ for which (35) vanishes. Substituting for s in (35) reveals that $P(s)$ has a zero when

$$\kappa^2\left[\frac{(\kappa-1)k_0^2t^2 4}{z^2}-1\right] = \tan^2(z/2). \tag{37}$$

Only one root exists when z is purely real; this root corresponds to the surface wave pole at $s_0=-\alpha_0$. The value of α_0 can be obtained graphically [17]. When α_0 is known, the residue R_0 can then be calculated from (13). The "leaky-wave" zeros of $P(s)$ correspond to values of z that are more generally complex and these roots will now be determined. From the form of (37) it is clear that if z_i is a root, z_i and $-z_i$ are also roots, and therefore only the first quadrant of the z plane need be investigated. By comparing the arguments of the right and left sides of (37) it can easily be shown that no "leaky-wave" roots exist in the first quadrant of the z plane unless Re $z \geq \pi$.

For any practical surface wave transmission system it is usually desirable to have most of the energy stored in the air immediately above the dielectric rather than in the dielectric itself in order that losses be kept to a minimum. The quantity $\kappa t\alpha_0$ gives a rough estimate of the ratio of electric energy stored in the dielectric to the energy in the air, per unit length of line. From the graphical solution of the transcendental equation (35) for α_0, it is obvious that $\kappa t\alpha_0$ can be made small by choosing

$$\sqrt{(\kappa-1)}\, k_0 t \ll \frac{\pi}{2}\cdot$$

Under such conditions and with the knowledge that $|z| \geq \pi$ for a root, it is clear that

$$\left|\frac{(\kappa-1)k_0^2 4t^2}{z^2}\right| \leq \frac{(\kappa-1)k_0^2 4t^2}{\pi^2} \ll 1 \qquad (38)$$

and thus this term can be neglected in (37). As an example, for the surface wave system employed in this work, $k_0 = 5.02$/inches, $\kappa = 2.54$, $t = 1/16$ inch, and thus

$$\frac{(\kappa-1)k_0^2 4t^2}{2} \doteq 0.06.$$

Making use of (38) in (37) and (36) gives

$$\tan(z/2) \doteq \pm j\kappa$$
$$s \doteq \pm j(z/2t). \qquad (39)$$

Eliminating z from these equations and solving for s gives the following expression for the "leaky-wave" roots:

$$s_n = \frac{1}{2t}\left[\ln\left(\frac{\kappa-1}{\kappa+1}\right) + jn\pi\right]$$
$$n = \pm 1, \pm 3, \pm 5, \cdots. \qquad (40)$$

Notice that the approximation associated with (38) improves with an increasing absolute value of n.

The residues of $R(s)$ are now easily found. At $s = s_n$ the numerator of (34) becomes

$$-P(-s_n) = 2\kappa s_n.$$

Note from (36) that

$$\frac{dz}{ds} = -\frac{(2t)^2 s}{z}\cdot$$

The derivative of $P(s)$ at s_n can thus be calculated as follows:

$$\frac{dP(s)}{ds}\Big/_{s=sn} = \frac{d}{ds}\left(s + \frac{z}{2t}\tan\frac{z}{2}\right)_{s=s_n}$$
$$= -t\frac{s}{z}\left[2\tan(z/2) + z + z\tan^2(z/2)\right]_{s=s_n}.$$

Using the approximate expressions (39), the residues are evaluated as

$$R_n = \frac{-P(-s_n)}{P'(s_n)} = \frac{2\kappa}{t(\kappa^2-1)} \qquad (41)$$

and these values are seen to be independent of the index n.

Substituting for the R_n, the sum over the "leaky-wave" poles in (32) can be written

$$\sum_{n=\pm 1,\cdots} R_n e^{s_n(y-y')} = \frac{2\kappa}{t(\kappa^2-1)}\left[\frac{\kappa-1}{\kappa+1}\right]^{(y-y')/2t} \sum_{n=-\infty}^{\infty} e^{j(2n+1)\pi(y-y')/2t}.$$

Recognizing the Fourier expansion of a periodic set of delta functions yields

$$\sum_{n=\pm 1,\cdots} R_n e^{s_n(y-y')} = \frac{2\kappa}{t(\kappa^2-1)} \sum_{n=-\infty}^{\infty}\left[\frac{1-\kappa}{1+\kappa}\right]^n \delta(y-y'+2nt). \qquad (42)$$

From (27) it is seen that $R(\infty) = (\kappa+1)/(\kappa-1)$. Using this result and (42) in (32) yields the desired representation for $g(y, 0)$, given by (36).

Acknowledgment

Special thanks are due Prof. R. S. Elliott who first suggested the problem. The generosity of the Lockheed California Company, Burbank, Calif., in supplying the surface wave table (Fig. 9) is also gratefully acknowledged.

References

[1] H. M. Barlow and J. Brown, *Radio Surface Waves*. London: Oxford, 1962.
[2] R. E. Collin, *Field Theory of Guided Waves*. New York: McGraw-Hill, 1960.
[3] F. J. Zucker, "Surface- and Leaky-wave Antennas," in *Antenna Engineering Handbook* compiled by H. Jasik, New York: McGraw-Hill, 1961, ch. 16.
[4] D. D. King and S. P. Schlesinger, "Losses in dielectric image lines," *IRE Trans. on Microwave Theory and Techniques*, vol. MTT-5, pp. 31–35, January 1957.
[5] R. H. DuHamel and J. W. Duncan, "Launching efficiency of wires and slots for a dielectric rod waveguide," *IRE Trans. on Microwave Theory and Techniques*, vol. MTT-6, pp. 277–284, July 1958.
[6] K. P. Sharma, "An investigation of the excitation of radiation by surface waves," *Proc. IEE (London)*, vol. 106B, pp. 116–122, March 1959.
[7] N. Marcuvitz, *Waveguide Handbook*, vol. 10, MIT Radiation Lab. Ser. New York: McGraw-Hill, 1951.
[8] J. W. Duncan and R. H. DuHamel, "A technique for controlling the radiation from dielectric rod waveguides," *IRE Trans. on Antennas and Propagation*, vol. AP-5, pp. 284–289, July 1957.
[9] J. R. Wait, "Two-dimensional treatment of mode theory of the propagation of VLF radio waves," *Radio Science, J. Res. NBS*, vol. 68D, pp. 81–93, January 1964.
[10] E. S. Gillespie, "An investigation of the scattering properties of strips above a surface wave system," Lockheed Aircraft Corp., L.R. 15019, January 1961.
[11] A. L. Cullen, "The excitation of plane surface waves," *Proc. IEE (London)*, vol. 101, pt. IV, pp. 225–234, February 1954.
[12] G. J. Rich, "The launching of a plane surface wave," *Proc. IEE (London)*, vol. 102, pt. III, pp. 237–246, March 1955.
[13] E. L. Ginzton, *Microwave Measurements*. New York: McGraw-Hill, 1957, pp. 235–293.
[14] F. E. Terman and J. M. Pettit, *Electronic Measurements*. New York: McGraw-Hill, 1952, pp. 145–147.
[15] N. Marcuvitz, "On field representations in terms of leaky modes or eigenmodes," *IRE Trans. on Antennas and Propagation*, vol. AP-4, pp. 192–194, July 1956.
[16] E. Jahnke and F. Emde, *Tables of Functions*. New York: Dover, 1945.
[17] R. Harrington, *Time-Harmonic Electromagnetic Fields*. New York: McGraw-Hill, 1961, pp. 163–171.